



1 **Investigating the synergistic potential Si and biochar to**
2 **immobilize soil Ni in a contaminated calcareous soil after *Zea***
3 ***mays* L. cultivation**

4 Hamid Reza Boostani¹, Ailsa G. Hardie², Mahdi Najafi-Ghiri¹, Ehsan Bijanzadeh³, Dariush
5 Khalili⁴, Esmaeil Farrokhnejad¹

6 ¹Department of Soil Science, College of agriculture and natural resources of Darab, Shiraz University, Darab74591,
7 Iran.

8 ²Department of Soil Science, Faculty of AgriSciences, Stellenbosch University, Private Bag X1, Matieland 7602,
9 South Africa

10 ³Department of agroecology, College of agriculture and natural resources of Darab, Shiraz University, Darab 74591,
11 Iran

12 ⁴Department of Chemistry, College of Sciences, Shiraz University, Shiraz 71454, Iran

13

14 *Correspondence to:* Hamid Reza Boostani (hr.boostani@shirazu.ac.ir)

15 **Abstract.** Silicon (Si) is a beneficial plant element that has been shown to mitigate the effects of
16 potentially toxic elements (PTEs) on crops. Biochar is a soil amendment that sequesters soil
17 carbon, and that can immobilize PTEs and enhance crop growth in soils. Considering these
18 beneficial properties, it remains to be investigated how the simultaneous utilization of Si and
19 biochars affects PTEs immobilization in soils. Therefore, the aim of this study was to examine the
20 interaction effects of Si levels and biochars, to alleviate soil Ni bioavailability and its
21 corresponding uptake in corn (*Zea Mays*) in a calcareous soil. A 90-day factorial greenhouse study
22 with corn was conducted. Si application levels were applied at 0 (S₀), 250 (S₁) and 500 (S₂) mg Si
23 kg⁻¹ soil and biochar treatments (3% wt.) included rice husk (RH) and sheep manure (SM) biochars
24 produced at 300°C and 500°C (SM300, SM500, RH300 and RH500). At harvest, corn shoot Ni-
25 concentrations, soil chemical Ni fractions and DPTA-release kinetics were determined.
26 Simultaneous utilization of Si and SM biochars led to a synergistic reduction (15-36%) of soluble
27 and exchangeable soil Ni fractions compared to application of Si (5-9%) and SM (5-7%) biochars
28 separately. The application of the Si and biochars also decreased DPTA-extractable Ni and corn
29 Ni shoot concentration (by up to 57%), with the combined application of SM500+S₂ being the
30 most effective. These effects were attributed to the transformation of Ni from more bioavailable
31 fractions to more stable iron oxide bound fractions, related to soil pH increase. The SM500 was
32 likely the most effective biochar due to its higher alkalinity and lower acidic functional group
33 content which enhanced Ni sorption reactions with Si. The study demonstrates the synergistic
34 potential Si and sheep manure biochar at immobilizing Ni in contaminated calcareous soils.

35 **1 Introduction**

36 One of the most important ways for potentially toxic elements (PTEs) to enter the human
37 food chain is the consumption of plants grown in soils contaminated with PTEs. Potentially toxic
38 elements pollute soil environments as a result of mining, metal smelting, using sewage sludge and
39 domestic and industrial effluents in agriculture especially in developing countries (Liu et al., 2018).
40 Soil PTEs cannot undergo biodegradation by living organisms, so they possess great stability and
41 longevity in the soil (Poznanović Spahić et al., 2019). Unlike other soil PTEs, such as mercury
42 (Hg), cadmium (Cd) and lead (Pb), nickel (Ni) is essential for plant growth at very low



43 concentrations. Nevertheless, at elevated contents (>35 mg Ni kg⁻¹ soil), it causes many
44 physiological and morphological malfunctions in plants and severely stunts their growth (Shahzad
45 et al., 2018; Antoniadis et al., 2017). Removing PTEs from contaminated sites is very expensive
46 and time-consuming, therefore, for plant cultivation in these areas, low-cost and effective methods
47 should be sought to stabilize soil PTEs and prevent them from being transferred to the plant (Gao
48 et al., 2023).

49 Silicon (Si) is a valuable nutrient for plant growth, and it is only considered essential for
50 some plant species such as rice. Applying Si to the soil can enhance plant resistance against
51 biological and non-biological tensions, including soil PTEs stress (Bhat et al., 2019; Yan et al.,
52 2018). It has been demonstrated in many studies that the soil application of Si for reducing plant
53 PTEs stress is more effective and economical than other remediating materials (Li, 2019; Adrees
54 et al., 2015). The application of Si in soils contaminated with PTEs may reduce the soil PTEs
55 bioavailability by increasing soil pH, increasing the secretion of organic ligands by the roots and
56 forming insoluble compounds with PTEs, and ultimately enhancing plant growth (Bhat et al.,
57 2019; Xiao et al., 2021).

58 Biochar is an organic soil amendment that sequesters soil carbon (C) that has received
59 much attention in recent years to stabilize PTEs in polluted sites (El-Naggar et al., 2018). Biochar
60 is a carbon-rich, porous organic material which is prepared in a limited or no oxygen conditions
61 by pyrolysis of organic wastes, including crop and animal residues, urban waste, wood by product
62 (Vickers, 2017; Ankita Rao et al., 2023). Addition of biochar to the soil not only improves the soil
63 chemical and physical properties, but also reduces the bioavailability of PTEs in contaminated
64 soils through some physicochemical processes such as sedimentation, complexation, and
65 electrostatic adsorption (Bandara et al., 2020; Deng et al., 2019; Derakhshan Nejad et al., 2018).
66 However, the efficiency of biochar prepared from different feedstocks and under different
67 production conditions in stabilizing soil PTEs can vary significantly (Dey et al., 2023).

68 Soil PTEs can exist in different chemical fractions such as water soluble and exchangeable
69 (WsEx), bound to carbonates (CAR), organic materials (OM), iron and manganese oxides
70 (FeMnOx) and residual (Res) (found in minerals) (Singh et al., 1988). The bioavailability of these
71 forms differs, as the WsEx fraction has the highest bioavailability and the Res form is considered
72 unusable by plants. The other chemical fractions of soil PTEs could be potentially accessible for
73 plant roots depending on soil characteristics (Kamali et al., 2011; Bharti et al., 2018). The quantity
74 and rate of release of soil PTEs from soil particles over time can influence their bioavailability.
75 Furthermore, the release kinetic parameters can provide insight into the mechanisms of soil PTEs
76 bonding and their potential risk for leaching into groundwater or surface water (El-Naggar et al.,
77 2021). Therefore, sequential extraction methods and release kinetics models have been employed
78 to assess the efficacy of amendment materials in stabilizing soil PTEs in contaminated soils. Xiao
79 et al. (2021) found that addition of mineral Si fertilizer to a contaminated paddy soil caused a
80 significant decrease in the Cd and Pb fractions bound to carbonates and iron-manganese oxides
81 while the forms of residual and bound to organic matter increased. In another study, application of
82 cotton residue biochar (1.5 wt. %) to a calcareous soil with a light texture containing different
83 levels of Cd contamination was more efficacious than corn and wheat straw biochars in decreasing
84 the WsEx-Cd and Car-Cd forms and enhancing the Res-Cd form. In addition, application of cotton
85 residue biochar decreased EDTA-extractable Cd by 45–52% compared to the control (Boostani et
86 al., 2023a).



87 As both biochars and Si are economical and effective soil amendments to reduce plant PTE
88 uptake and stress in contaminated soils, it remains to be investigated how their combined
89 application affects the chemical fractions and release kinetics of Ni in calcareous soils. Currently,
90 no previous studies have investigated their interactive effects on soil PTEs immobilization. The
91 primary objective of the present study was to elucidate the interaction of biochars and Si levels, to
92 alleviate soil Ni bioavailability and its corresponding accumulation in corn (*Zea Mays* L. 604)
93 plant. Additionally, the study sought to elucidate the underlying soil chemical mechanisms that
94 are likely to be responsible for such effects.

95 **2 Materials and methods**

96 2.1 Soil sampling, polluting and its characteristics

97 A composite soil sample from the surface layer (0-30 cm) was collected at the research
98 farm of the College of Agriculture and Natural Resources in Darab, southern Iran. The soil sample
99 was air-dried, sieved through a 2 mm mesh, and subjected to standard laboratory methods for the
100 measurement of various physicochemical soil properties (Page et al., 1982). Plastic containers
101 were filled with soil samples, each weighing two kilograms and then 300 mg Ni kg⁻¹ soil supplied
102 as Ni(Cl₂) solution was added to them using the method that previously described by Boostani et
103 al. (2023c).

104 2.2 Production of biochar and its properties

105 After air-drying and pulverizing of the feedstocks, rice husk and sheep manure, a slow
106 pyrolysis procedure (2 h at 300°C and 500°C) in an oxygen-limited environment was carried out
107 to generate biochars (Anand et al., 2023). The generated biochars were then cooled at ambient
108 temperature and sieved with a 0.5 mm mesh to ensure consistent particle size. The chemical
109 characteristics of the biochars were assessed using the methods outlined in Boostani et al. (2023b).

110 2.3 Greenhouse experiment

111 A completely randomized factorial experiment was conducted in a greenhouse
112 environment with three replications. The first factor consisted of the biochar treatments including
113 rice husk and sheep manure generated at 300°C and 500°C (SM300, SM500, RH300 and RH500),
114 each at the rate of 3% wt. the second factor included Si application levels (0 (S₀), 250 (S₁) and 500
115 (S₂) mg Si kg⁻¹ soil) supplied as Na₂SiO₃ solution. Based on the experimental design, Si levels
116 were added to the 2 kg of contaminated soil samples and after drying the soil and mixing it, the
117 prepared biochars were added to the required amount. Immediately after that, the treated soil
118 samples were transferred to plastic pots and to facilitate the required reactions, the moisture content
119 of the samples was kept at field capacity level for a duration of two weeks. Thereafter, 6 corn seeds
120 (*Zea mays* L. 604) were planted in each pot, and at the 4-leaf stage, 2 plants were kept in each pot
121 until the end of cultivation. During the growth of the plant, distilled water was used to maintain
122 the soil moisture content in the pots at field capacity. After 90 days, the plants were harvested at
123 the soil interface, rinsed with distilled water to remove contamination, immediately air-dried and
124 kept for Ni determination of plant shoots. After separating the roots and air drying, the soil of the
125 pots was sifted via a 2 mm mesh, and subsequently utilized for performing Ni release kinetics
126 experiment and determining the Ni chemical fractions.

127 2.4 Sequential extraction procedure



128 The present study employed a successive extraction technique (Singh et al., 1988) to
 129 fractionate soil nickel (Ni) in the following chemical forms, namely water-soluble and
 130 exchangeable (WsEx), carbonate-bound (Car), organic matter-bound (OM), manganese oxide-
 131 bound (MnOx), amorphous iron oxide-bound (AFeOx), crystalline iron oxide-bound (CFeOx), and
 132 residual (Res). The methodological specifics are provided in Table 1.

Table 1
 Successive extraction technique of Singh et al. (1988)

Chemical speciation containing Ni	acronym	Duration of agitation (h)	Extractants	Relative density (g.cm ⁻³)
Exchangeable and soluble	WsEx	2	1 M magnesium nitrate	1.10
Carbonate	Car	5	1 M sodium acetate (pH=5)	1.04
Organic	OM	0.5	0.7 M sodium hypochloride (pH=8.5)	1.00
Mn oxide	MnOx	0.5	0.1 M hydroxyl amine hydrochloride (pH=2 by nitric acid)	1.00
Amorphous Fe oxides	AFeOx	0.5	0.25 M hydroxyl amine hydrochloride + 0.25 M chloridric acid	1.01
Crystalline Fe oxides	CFeOx	0.5	0.2 M ammonium oxalate + 0.2 M oxalic acid + 0.1 M ascorbic acid	1.02

133

134 2.5 Release kinetics experiment

135 Fifty milliliters centrifuge tube was filled with ten grams of soil. After that, the soil sample
 136 was supplemented with 20 ml of DTPA solution (pH: 7.3) (Lindsay and Norvell, 1978). The soil-
 137 DTPA mixture were stirred (125 rpm) for specific periods of time, i.e. 5, 15, 30, 60, 120, 360, 720
 138 and 1440 minutes at a constant temperature (25 ± 2 °C). After each stirring time, the soil suspension
 139 was filtered to separate the soil particles from the liquid phase. Atomic absorption spectroscopy
 140 (AAS) (PG 990, PG Instruments Ltd. UK) was used to analyze the Ni concentration in the liquid
 141 phase. The Ni concentration in the liquid phase versus time was plotted to obtain a Ni release
 142 kinetic curve. A total of seven kinetic models namely order models (zero, first, second and third),
 143 parabolic diffusion, power function and simple Elovich were assessed to fit the Ni release data.
 144 The best models for describing the data were selected according to the maximum value of the
 145 coefficient of determination (R^2) and the minimum amount of the standard error of estimate
 146 (SEE)(Nasrabadi et al., 2022).

147 2.6 Data analysis

148 The ANOVA test was utilized to assess treatments effects in the individual and combined
 149 application. Additionally, a comparison of means was conducted using the MSTATC computer
 150 program, applying Duncan's test with a significance level of 5%. The charts were generated using
 151 the software Excel 2013. The Pearson correlation coefficients among the dataset was determined
 152 using SPSS 12.0.

153 3 Results and Discussions

154 3.1 Soil characteristics



155 The uncontaminated soil exhibited a sandy loam texture and possessed alkaline properties
156 with significant calcium carbonate content, while not being classified as saline (Table 2). The
157 quantity of soil organic matter was extremely low, a distinct characteristic of soils from arid and
158 semi-arid regions (Okolo et al., 2023) (Table 2). The relatively low levels of clay and organic
159 matter present in the soil contributed to a correspondingly low soil cation exchange capacity (CEC)
160 (Table 2). Furthermore, it should be noted that the concentration of soil Ni extractable by
161 diethylene triamine penta acetic acid (DTPA) was very low (Table 2).

Table 2
Certain physicochemical attributes of the soil prior to cultivation.

Sand (%)	58.0
Silt (%)	30.0
Clay (%)	12.0
Soil textural class	Sandy loam
pH _(s)	7.59
EC (dS m ⁻¹)	2.60
CCE (%)	55.0
OM (%)	0.50
CEC (cmol ₍₊₎ kg ⁻¹)	11.7
Ni-DTPA (mg kg ⁻¹)	0.39

Notes: EC, electrical conductivity; OM, organic matter; CCE, calcium carbonate equivalent; CEC, cation exchange capacity.

162

163 3.2 Chemical characteristics of the biochars

164 As the pyrolysis temperature rose from 300 °C to 500 °C, the SM biochars demonstrated
165 elevated pH and EC values, with the highest levels observed at the highest temperature (Table 3).
166 The elevated levels of alkali salts, which are reflected in the high ash content (Table 3), are the
167 contributing factor behind this observation in the SM biochars in comparison to the RH biochars.
168 Plant-based biochars commonly exhibit reduced levels of dissolved solids in comparison to
169 animal-based biochars (Sun et al., 2014). The SM300 biochar possessed the highest CEC value of
170 19.70 cmol₍₊₎ kg⁻¹. The observed phenomenon may be attributed to the diminution of surface
171 functional groups, namely carboxyl and phenol, at elevated pyrolysis temperatures. These groups
172 are predominantly responsible for facilitating the cation exchange capacity (CEC) of biochars
173 (Tomczyk et al., 2020). As the pyrolysis temperature increased, there was an observed increase in
174 the C content of the biochars, and a corresponding decrease in the content of hydrogen, oxygen,
175 and nitrogen (Table 3). The observed increase in the concentration of C as pyrolysis temperature
176 rises is consistent with a concomitant rise in the degree of carbonization. The observed reduction
177 in the levels of H and O might be attributed to the occurrence of dehydration reactions,
178 decomposition of oxygenated bonds, and the liberation of low molecular weight byproducts rich
179 in H and O, as recently noted by Zhao et al. (2017). Nitrogen compound volatilization explains the
180 diminished N content of the biochars at elevated pyrolysis temperatures. The ratios of H:C and
181 O:C are significant indicators of the aromaticity and polarity of biochars (Chatterjee et al., 2020).
182 The results of Table 3 indicate that the H:C and O:C mole ratios showed a gradual decrease as the
183 pyrolysis temperature was increased, which can be interpreted as a sign of improved carbonization
184 of the biochars (Zhao et al., 2017). The results indicated that the Ni content in the biochars derived



185 from rice husk was insignificant. However, a limited quantity of Ni was detected in the biochars
186 produced from sheep manure, as illustrated in Table 3.

Table 3
Some physical and chemical properties of the biochars.

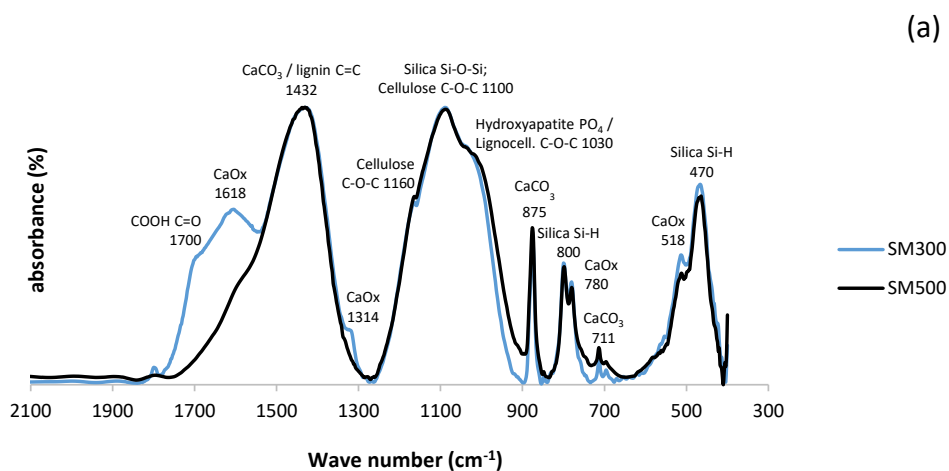
	SM300	SM500	RH300	RH500
pH (1:20)	9.96	11.0	9.0	10.3
EC (1:20) (dS m ⁻¹)	3.94	4.28	0.84	1.17
CEC (cmol. kg ⁻¹)	19.70	18.94	18.94	15.33
C (%)	25.4	31.8	45.0	50.0
H (%)	1.85	0.8	2.28	1.06
N (%)	2.10	1.57	1.30	1.10
Ni (mg kg ⁻¹)	3.0	15.4	Nd	Nd
Moisture content (%)	1.91	1.82	2.65	2.37
Ash content (%)	53.8	60.0	34.2	44.8
H:C mole ratio	0.87	0.30	0.60	0.25
O+S:C mole ratio	0.44	0.09	0.24	0.01

Notes: SM300, sheep manure biochar generated at 300 °C; SM500, sheep manure biochar generated at 500 °C; RH300, rice husk biochar produced at 300 °C; RH500, rice husk biochar produced at 500 °C; CEC, cation exchange capacity; EC, electrical conductivity; Nd, non-detectable.

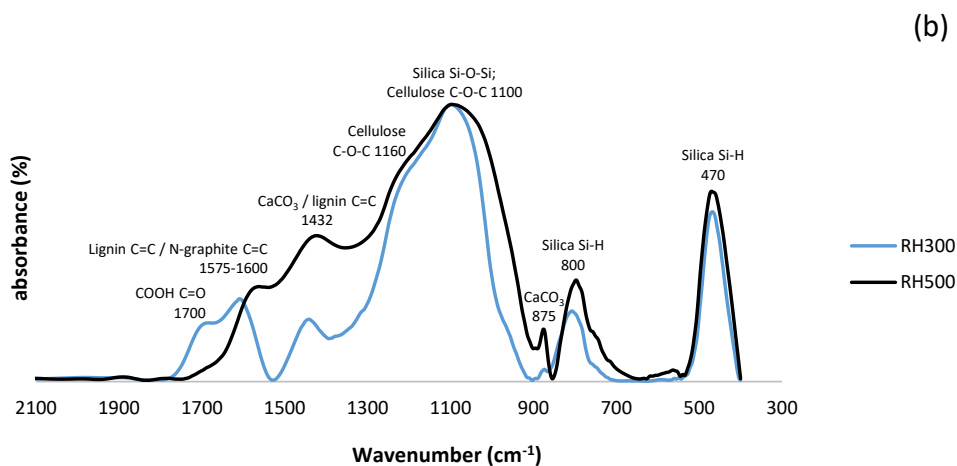
187

188 3.3 FTIR and SEM of the biochars

189 The FTIR spectra of the SM and RH biochars are shown in Figure 1. The SM and RH
190 biochars produced at 300 °C contained a higher content of carboxyl groups (1700 cm⁻¹) (Keiluweit
191 et al., 2010) than the biochars produced at 500 °C, which is in agreement with the O:C values of
192 the biochars (Table 2). All of the biochars contained absorption bands associated with lignin (1430
193 cm⁻¹) and cellulose (1030 -1160 cm⁻¹) (Keiluweit et al., 2010). The SM biochar contained more
194 calcite than the RH biochar as evident by the greater intensity of calcite characteristic peaks at
195 1432, 875, and 711cm⁻¹ (Myszka et al., 2019) in the SM biochars (Fig. 1a). There was also
196 evidence of the presence of Ca oxalate in the SM biochars, indicated by the characteristic peaks at
197 1618, 780 and 518 cm⁻¹ (Maruyama et al., 2023). All the biochars contained silica as evident by
198 the intense silica absorption peaks at 1100, 800 and 470 cm⁻¹ (Zemnukhova et al., 2015).



199

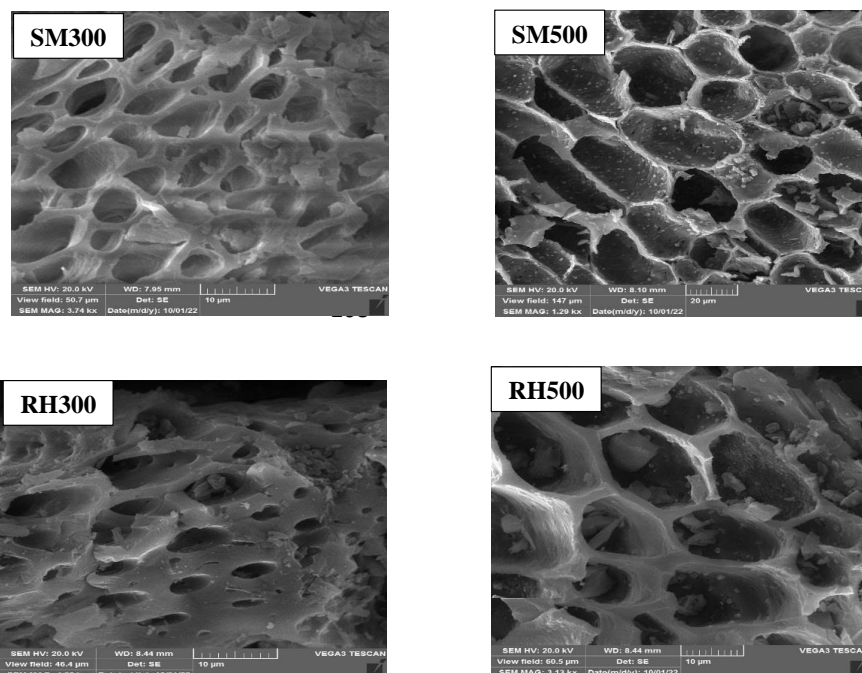


200

201 **Fig. 1.** FTIR of the biochars in the wave number range of 400-2000 cm⁻¹. Notes: SM300, sheep manure
202 biochar produced at 300°C; SM500, sheep manure biochar produced at 500°C; RH300, rice husk biochar produced at
203 300°C; RH500, rice husk biochar produced at 500°C.

204

205 The SEM images of the SM and RH biochars are shown in Figure 1. The morphology of
206 the biochars became more rigid and porous at higher temperatures, as evidenced by the cell wall
207 shrinkage attributed to devolatilization of organic tissues (Claoston et al., 2014).

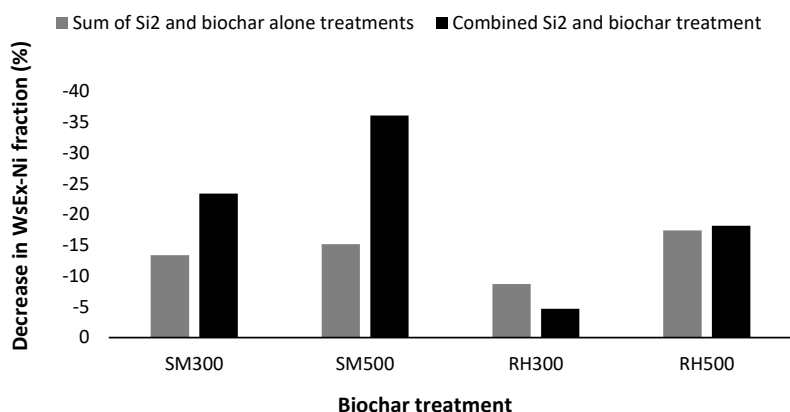


209

210 **Fig. 2.** SEM of the biochars. Notes: SM300, sheep manure biochar produced at 300°C; SM500, sheep manure
211 biochar produced at 500°C; RH300, rice husk biochar produced at 300°C; RH500, rice husk biochar produced at 500°C.
212

213 3.4 Soil Ni chemical fractions as affected by Silicon levels and biochars

214 The main effects of treatments (biochars and Si levels) and their interactions (except for
215 the Ni-Car fraction) on the content of soil Ni chemical fractions were statistically significant
216 ($P < 0.01$). The soil Ni concentration in the WsEx fraction was significantly reduced by the
217 application of Si rates from S_0 to S_2 by 14.8% (Table 4). Among the biochar treatments, the greatest
218 decrease in WsEx-Ni fraction compared to the control was due to SM500 by 17%, while the
219 RH300 treatment had no significant effect (Table 4). The interaction effect of treatments indicated
220 that the lowest WsEx-Ni concentration was due to the combined treatment of SM500+ S_2 (4.04 mg
221 Ni kg^{-1} soil) (Table 4). The combined treatment of S_2 and SM biochars had strong synergistic effect
222 on reducing WsEx-Ni fraction (23-36% reduction) compared to the sum of the treatments alone
223 (13-15% reduction) (Fig. 3). Whereas this synergistic effect of the combined treatments was not
224 evident for the RH biochars (Fig. 3). There was a negative correlation between soil WsEx fraction
225 and soil pH ($r = -0.66$, $p < 0.01$). The addition of biochar and silicon result in increases in soil
226 pH, and affect the bioavailability of PTEs and their conveyance to plant roots (Shen et al., 2020;
227 Ma et al., 2021). Among the applied biochars, the maximum and minimum pH and ash content
228 were attributed to the SM500 and RH300, respectively (Table 3). Furthermore, SM biochars
229 contained substantially more calcite than the RH biochars (Fig. 1). The combined SM500+ S_2 was
230 most effective at reducing WsEx-Ni fraction, likely due to the higher alkalinity and lower acidic
231 functional group content of SM500, which resulted in the greatest soil pH increases, promoting Ni
232 precipitation and adsorption (Sachdeva et al. 2023).



233

234 **Fig. 3.** Comparison of the effect of sum of the Si₂ and biochar alone treatment versus the combined
 235 Si₂ and biochar treatments on the % reduction of the WsEx-Ni fraction. Notes: SM300, sheep manure
 236 biochar produced at 300 °C; SM500, sheep manure biochar produced at 500 °C; RH300, rice husk biochar produced at
 237 300 °C; RH500, rice husk biochar produced at 500 °C.

238 The reduced effectiveness of biochars produced at 300 °C, as compared to those produced
 239 at 500 °C, in decreasing soil Ni-WsEx content may also be attributed to the lower rates of microbial
 240 oxidation and mineralization of RH500 and SM500, which is indicated by their higher
 241 environmental stability (as reflected by lower H/C mole ratio values) (Table 3). Consequently,
 242 biochar produced at 500 °C may not provide sufficient acidic carboxyl functional groups to the
 243 soil to stimulate SOM decomposition, leading to a greater increase in soil pH (Sun et al., 2023).
 244 According to Zhu et al. (2015), the addition of wine lees-based biochar (a material from a wine
 245 processing factory) to a heavy metal-contaminated soil (at rates of 0.5% and 1% w/w) resulted in
 246 an increase in soil pH and a decrease in the soil Ni content in the WsEx fraction. Furthermore, the
 247 increase in soil pH due to the increase in Si levels may lead to the precipitation of Ni in the forms
 248 of Ni silicate and hydroxide. Due to the high solubility of Na metasilicate, the hydrolysis of silicate
 249 anion in the soil solution is intensified, leading to a high concentration of OH⁻ and a subsequent
 250 increase in soil pH (Ma et al., 2021).

Table 4

Effects of biochars and silicon levels on the soil Ni chemical fractions (mg kg⁻¹) and Ni mobility factor (%) after corn cultivation.

	C	SM300	SM500	RH300	RH500	
	WsEx					
S ₀	6.32 a	6.02 a-c	5.91 bc	6.31 a	5.77 c	6.07 A
S ₁	6.03 a-c	5.37 d	5.09 de	6.25 ab	5.28 d	5.60 B
S ₂	5.77 c	4.84 e	4.04 f	6.02 a-c	5.17 de	5.17 C
Mean	6.04 A	5.41 B	5.01 C	6.20 A	5.41 B	
	OM					
S ₀	9.72 a	10.15 a	8.04 d-f	10.08 a	9.02 b	9.40 A
S ₁	9.60 a	9.75 a	7.16 g	8.62 b-d	8.70 bc	8.76 B
S ₂	8.11 c-f	7.94 ef	7.12 g	8.30 c-e	7.63 fg	7.82 C
Mean	9.14 A	9.28 A	7.44 C	8.99 A	8.44 B	
	MnOx					
S ₀	11.58 a	3.77 kl	5.99 f	4.69gh	9.71 c	7.15 A



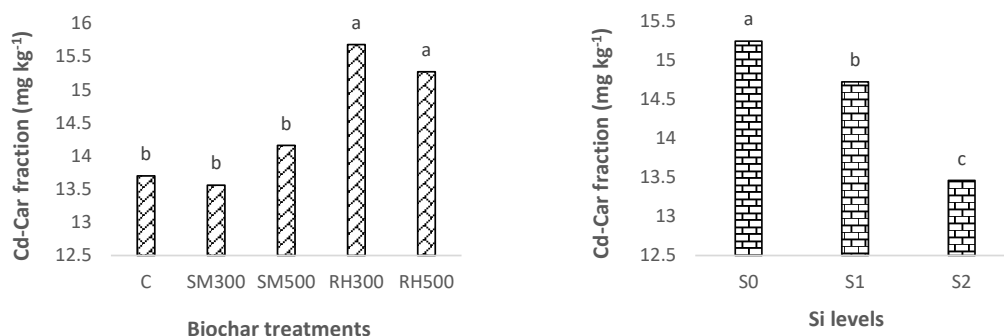
S ₁	10.33 b	3.50 l	5.00 g	4.57 hi	8.93 d	6.48 B
S ₂	10.28 b	2.98 m	4.28 ij	3.96 jk	7.94 e	5.89 C
Mean	10.73 A	3.42 E	5.09 C	4.41 D	8.86 B	
AFeOx						
S ₀	11.15 ef	10.38 g	11.83 d	10.96 fg	11.75 de	11.21 C
S ₁	12.20 b-d	10.73 fg	12.03 cd	12.20 b-d	12.66 bc	11.96 B
S ₂	12.84 b	12.18 b-d	12.16 b-d	12.31 b-d	14.25 a	12.74 A
Mean	12.06 B	11.09 C	12.00 B	11.82 B	12.88 A	
CFeOx						
S ₀	77.32 f	77.98 f	83.97 cd	84.67 cd	79.60 ef	80.67 C
S ₁	77.89 f	82.20 de	86.34 bc	85.12 b-d	83.62 cd	83.03 B
S ₂	79.92 ef	85.50 bc	87.88 ab	85.69 bc	90.40 a	85.88 A
Mean	78.37 C	81.89 B	86.00 A	85.16 A	84.54 A	
Res						
S ₀	199.7 c-e	207.5 a	199.8 c-e	196.5 f	197.8 d-f	200.3 A
S ₁	199.9 c-e	204.5 b	200 cd	197.3 ef	195.5 f	199.5 A
S ₂	200.3 cd	204.1 b	201 c	199.4 c-e	190.4 g	199 A
Mean	200 B	205.4 A	200.3 B	197.7 B	194.6 BC	

Notes: C, control; SM300, sheep manure biochar produced at 300°C; SM500, sheep manure biochar produced at 500°C; RH300, rice husk biochar produced at 300°C; RH500, rice husk biochar produced at 500°C; S₀, without Si addition; S₁, application of 250 mg Si kg⁻¹ soil; S₂, application of 500 mg Si kg⁻¹ soil. WsEx, water soluble and exchangeable fraction; OM, organic fraction; MnOx, bound to manganese oxides; AFeOx, bound to amorphous iron oxides; CFeOx, bound to crystalline iron oxides; Res, residual fraction; MF, mobility factor.

* Numbers followed by same letters in each column and rows, in each section, are not significantly (P<0.05) different

251 Application of Si rates from S₀ to S₂ significantly decreased the soil Ni content in the Car
 252 fraction by 11.70% (Figure 4). The SM biochars had no significant effect on the Car-Ni fraction
 253 whereas addition of RH biochars led to a significant increase in this fraction (Figure 4). Ippolito
 254 et al. (2017) found that addition of two biochars (pine [*Pinus contorta*] and tamarisk [*Tamarix*
 255 spp.]) to a mine contaminated soil caused a significant increase in the soil Cd content bound to
 256 carbonates. They concluded that the reduction in Cd bioavailability may have been due to the
 257 ability of biochar to raise soil pH levels and induce the precipitation of CdCO₃. Similarly, Yuan et
 258 al. (2011) proposed that the decrease in soil PTEs bioavailability might have been caused by the
 259 creation of metal-carbonate species and carbonate-surface functional group reactions, which could
 260 function as a mechanism for sequestration. The decrease in the concentration of Ni in the carbonate
 261 form with an increase in the Si levels could potentially be explained by the competition between
 262 silicate (SiO₄⁻⁴) and carbonate ions for binding with Ni⁺² ions in the soil solution.

263



264

265 **Fig. 4.** Effects of (a) biochars and (b) silicon levels on the soil Ni concentration (mg kg⁻¹) in the
 266 carbonate-bound fraction after corn cultivation. Notes: C, control; SM300, sheep manure biochar produced
 267 at 300°C; SM500, sheep manure biochar produced at 500°C; RH300, rice husk biochar produced at 300°C; RH500,
 268 rice husk biochar produced at 500°C; S₀, without Si addition; S₁, application of 250 mg Si kg⁻¹ soil; S₂, application of
 269 500 mg Si kg⁻¹ soil. * Numbers followed by same letters in each section, are not significantly (P<0.05) different.

270

271 The biochars produced at 300°C had no significant effect on the OM-Ni fraction compared
 272 to control, while the biochars generated at 500°C significantly decreased it (Table 4). The greatest
 273 OM-Ni reduction (18.6%) was due to SM500. Lu et al. (2017) explored how the application of
 274 bamboo and rice straw biochars with varying mesh sizes (0.25 and 1 mm) and at three different
 275 rates (0, 1, and 5% w/w) affected the distribution of Cd in a contaminated sandy loam soil, using
 276 the BCR sequential extraction method. They reported that changes in the concentration of the Cd-
 277 OM fraction as affected by the biochars varied depending on the type, mesh size, and application
 278 rate of the biochar. In another study, the application of sheep manure biochar produced at 500°C
 279 at the rate of 3% (w/w) to a Cd-contaminated calcareous soil resulted in a significant increase in
 280 the OM-Cd fraction, whereas the addition of other biochar treatments (wheat straw, corn straw,
 281 rice husk, licorice root pulp) caused a significant decrease in the concentration of Cd in the OM
 282 form when compared to the control soil (Boostani et al., 2018). By increasing the Si rates from S₀
 283 to S₂, the OM-Ni fraction was reduced by 16.8% (Table 4). It has been shown that the application
 284 of Si to cultivated soils resulted in a reduction of soil organic matter content. This implies that Si
 285 facilitates the decomposition and accessibility of organic matter to plants (Ma et al., 2021). The
 286 interaction effects of biochars and Si levels showed that the lowest OM-Ni concentration was due
 287 to the combined treatment of SM500+S₂ (7.12 mg Ni kg⁻¹ soil), which was equal to a 26.7%
 288 decrease compared to the combined treatment of C+S₀ (9.72 mg Ni kg⁻¹ soil) (Table 4).

289 All the biochar treatments caused a significant decrease in MnOx-Ni fraction compared to
 290 control, with the greatest reduction was attributed to the SM300 by 52.6% (Table 4). The lower
 291 temperature biochars were more effective than the higher temperature biochars in decreasing the
 292 MnOx-Ni fraction (Table 4). Furthermore, the addition of Si rates from S₀ to S₂ significantly
 293 decreased MnOx-Ni by 17.6% (Table 4). The interaction effect of treatments showed that the
 294 highest and the lowest MnOx-Ni concentrations were due to the combined treatments of C+S₀
 295 (11.58 mg Ni kg⁻¹ soil) and SM300+S₂ (2.98 mg Ni kg⁻¹ soil), respectively (Table 4). The



296 concentrations of soil Ni bound to AFeOx and CFeOx were significantly increased by application
297 of Si levels from S₀ to S₂ by 13.6% and 6.5%, respectively (Table 4). Belton et al. (2012)
298 demonstrated that exogenous silicon application resulted in the attachment of silicate to the surface
299 of iron oxide in the form of a polymer. Following the complexation of ferrosilicon, a significant
300 number of negatively charged functional groups, including silanol, were formed. These groups
301 provided numerous adsorption sites for soil PTEs, ultimately reducing their bioavailability (Belton
302 et al., 2012). In general, all the biochars caused a significant increase in CFeOx-Ni fraction, and
303 there were no significant differences among the SM500, RH300 and RH500 treatments (Table 4).
304 However, the only the RH500 treatment increased the AFeOx-Ni concentration of soil compared
305 to control (Table 4). Among all the biochars, only the SMB300 resulted in a significant increase
306 in the soil Ni concentration in the Res fraction compared to the control (Table 4). The application
307 of Si also did not significantly effect this form (Table 4).

308 Mailakeba and Bk (2021) studied the addition of kunai grass biochar (0.75%) to a soil with
309 different Ni contamination levels (0, 56, 100, and 180 mg Ni kg⁻¹ soil). They found that the
310 application of the grass biochar increased the Res-Ni fraction and reduced the WsEx and OM-Ni
311 fractions. In another study, Boostani et al. (2023c) demonstrated that the application of biochars
312 (cow manure, municipal compost and licorice root pulp each at 3%(w/w)) to a Ni-contaminated
313 soil increased the concentrations of OM-bound and residual Ni fractions, and decreased the
314 concentrations of WsEx, Car, and Fe/Mn oxide-bound Ni fractions. Whereas, Boostani et al.
315 (2023b) found that the application of manure and compost biochars (3% w/w) to Pb-contaminated
316 soil did not significantly affect the Res-Pb fraction but did decrease the WsEx fraction. Therefore,
317 it seems that the effect of biochars on the transformation of soil PTE chemical fractions depends
318 on the raw materials and production conditions of the biochar, the soil application rates, type of
319 PTEs, the degree of soil contamination with PTEs, the selection of sequential extraction procedure
320 and the soil properties (Mailakeba and Bk, 2021; Boostani et al., 2023a, b; Boostani et al., 2021).

321 In summary, the application of biochars in the present study resulted in the transformation
322 of Ni in the soil from more bioavailable and mobile fractions (WsEx, MnOx, OM) to more stable
323 forms (AFeOx and CFeOx). These changes were particularly evident in the WsEx fraction when
324 SM biochar was applied in conjunction with silicon, indicating that the simultaneous use of these
325 two substances was much more effective than applying them separately.

326 3.5 Shoot Ni concentration of *Zea mays* L. as affected by treatments

327 The main effects of biochars, Si rates and their interactions were statistically significant on
328 the shoot Ni concentration of the corn. Addition of Si levels from S₀ to S₂ resulted in 32% decrease
329 in shoot Ni concentration (Table 5). In addition, the shoot Ni concentration was significantly
330 decreased by application of all the biochar treatments compared to the control (with no biochar
331 addition) (Table 5). Only the RH500 and SM300 treatments differed statistically from each other.
332 The interaction effects of treatments showed that the highest and lowest shoot Ni concentration
333 were due to the combined treatments of C+S₀ (10.4 mg Ni kg⁻¹ DM) and SM500+S₂ (4.45 mg Ni
334 kg⁻¹ DM), respectively (Table 5). The shoot Ni concentration had a significant and positive
335 correlation with the Ni-WsEx fraction ($r = +0.62, P < 0.01$) while there were a significant and
336 negative correlation between the soil pH ($r = -0.60, P < 0.01$) and Ni-CFeOx fraction ($r =$
337 $-0.50, P < 0.01$). This indicates that the application of Si and biochar can reduce the shoot Ni
338 concentration by increasing soil pH and, as a result, reducing the amount of Ni in the fraction of
339 WsEx and increasing the Ni content attached to crystalline iron oxides. Boostani et al. (2019a)



340 reported the reduction of shoot Ni concentration of spinach (*Spinacia oleracea* L.) due to the
 341 application rice husk and licorice root pulp biochars (2.5% w/w) application in a Ni-contaminated
 342 calcareous soil. Additionally, they reported that the biochars produced at 350 °C were more
 343 effective at reducing crop Ni uptake and promoting plant growth than the biochars produced at
 344 550 °C. The most significant factors that contribute to the reduction of PTE-uptake by plants in
 345 contaminated soils that have been amended with biochars include surface adsorption of heavy
 346 metals, increased soil pH, altered redox conditions of PTEs, improved physical and biological
 347 properties of the soil, changes in the activity levels of antioxidant enzymes, and a decrease in the
 348 transfer of PTEs to the plant shoots (Zeng et al., 2018; Rizwan et al., 2016). Several studies have
 349 investigated the effect of soil Si application on shoot Ni concentration in various plant species.
 350 Some studies have reported that the application of Si to soil resulted in a reduction of shoot Ni
 351 concentration, while others have found no significant effect (Ma and Yamaji, 2006; Flore et al.,
 352 2012). One possible explanation for the reduction in shoot Ni concentration is that Si can compete
 353 with Ni for uptake by plant roots. Silicon has a similar ionic radius to Ni, which means that it can
 354 occupy the same binding sites on root cell membranes and reduce the uptake of Ni. Additionally,
 355 Si can induce the expression of genes that are involved in Ni transport and homeostasis, which
 356 may contribute to the reduced shoot Ni concentration (Hossain et al., 2012; Liang et al., 2005).

Table 5

Shoot Ni concentration (mg Ni kg⁻¹ DM) as affected by biochars and silicon application levels.

	C	SM300	SM500	RH300	RH500	
S ₀	10.4 a	7.35 bc	9.85 a	7.55 bc	7.65 b	8.56 A
S ₁	7.65 b	6.90 bc	6.60 cd	7.05 bc	7.35 bc	7.11 B
S ₂	7.20 bc	5.05 ef	4.45 f	5.80 de	6.60 cd	5.82 C
Mean	8.41 A	6.43 C	6.96 BC	6.80 BC	7.20 B	

Notes: C, control; SM300, sheep manure biochar generated at 300 °C; SM500, sheep manure biochar generated at 500 °C; RH300, rice husk biochar produced at 300 °C; RH500, rice husk biochar produced at 500 °C; S₀, without Si application; S₁, addition of 250 mg Si kg⁻¹ soil; S₂, addition of 500 mg Si kg⁻¹ soil.

357

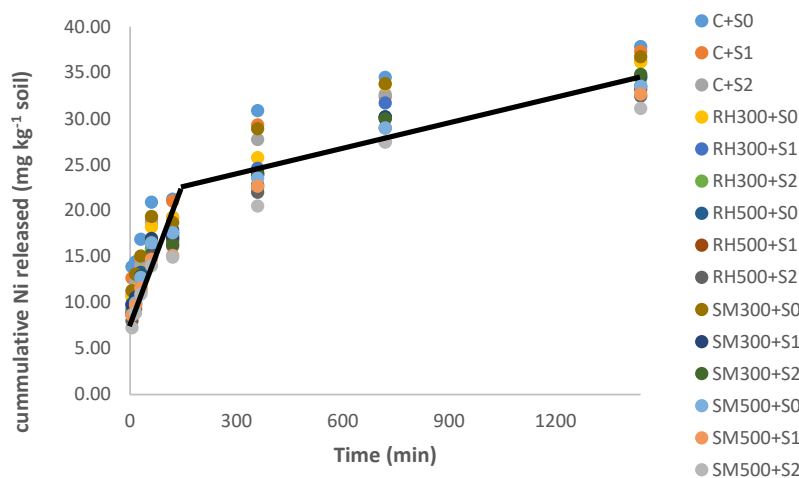
358 3.6 Soil Ni desorption as affected by Silicon levels and biochars

359 The cumulative soil Ni desorption (extracted by DTPA) as a function of time are shown in
 360 Fig. 5. The release of Ni from the soil initially proceeded at a much higher rate during the first
 361 hour, and then proceeded at a much slower rate during the next 24 hours, as illustrated by the trend-
 362 line in Fig. 5. This two-stage process of releasing heavy metals from soil has also been reported
 363 by other researchers (Sajadi Tabar and Jalali, 2013; Boostani et al., 2023a). It is likely that the
 364 first stage of release is related to forms of Ni that are less strongly attached to soil particles,
 365 including WsEx and Car, while the second stage of desorption is likely from fractions of Ni with
 366 less bioavailability, such as FeOx and Res (Saffari et al., 2015). In general, the amount of soil Ni
 367 desorption was reduced by addition of biochars and Si levels (Fig. 5). In addition, the effects of
 368 biochars produced at higher pyrolysis temperature (500 °C) on reducing the soil Ni release was
 369 more than those generated at lower pyrolysis temperature (300 °C). The highest amount of soil Ni
 370 release was due to the combined treatment of C+S₀ (37.84 mg Ni kg⁻¹ soil) while the lowest was
 371 observed in the combined application of SM500 and S₂ (31.13 mg Ni kg⁻¹ soil) treatment.

372



373



374

375 **Fig. 5.** Cumulative soil Ni desorption (extracted by DTPA) (mg kg^{-1}) as affected by different
 376 treatments. Notes: C, control; SM300, sheep manure biochar produced at 300°C ; SM500, sheep manure biochar
 377 produced at 500°C ; RH300, rice husk biochar produced at 300°C ; RH500, rice husk biochar produced at 500°C ; S₀,
 378 without Si addition; S₁, application of $250 \text{ mg Si kg}^{-1}$ soil; S₂, application of $500 \text{ mg Si kg}^{-1}$ soil.

379 **3.7 Fitting of Ni release data to kinetics models**

380 The soil Ni release data during 24 hours for all the biochar and Si treatments were evaluated
 381 by seven different kinetic models (Table 6). The effectiveness of the various kinetic models to
 382 describe the observed soil Ni desorption was analyzed by considering the coefficient of
 383 determination (R^2) and standard error of estimate (SEE), so that the highest value of the R^2 and the
 384 lowest value of the SEE were set as the criteria. As seen in Table 6, the order kinetic models did
 385 not adequately describe soil Ni release, and with the increase in the order of the kinetic model
 386 (from zero to third), the value of the R^2 decreased. This has also been found by other researchers
 387 for the release of heavy elements from soil (Boostani et al., 2019b; Ghasemi-Fasaei et al., 2006).
 388 Whereas, the non-order kinetic models, including power function, parabolic diffusion and simple
 389 Elovich, acceptably described the soil Ni release of the various treatments (Table 6). Among them,
 390 the power function model was the best according to the highest value of R^2 (0.98) and the lowest
 391 value of SEE (0.055). Boostani et al. (2018) also reported that the power function was the best
 392 kinetic model to describe soil Cd desorption from a Cd-contaminated soil treated with biochars
 393 and zeolite.

394

395

396

397



Table 6

The range of coefficients of determination (R^2) and standard error of estimate (SEE) of applied kinetic models to all the soil treatments.

Kinetic models	R^2		SEE	
	Range	Mean	Range	Mean
Zero order	0.79-0.87	0.80	3.36-4.67	3.67
First order	0.69-0.75	0.75	0.22-0.29	0.25
Second order	0.53-0.61	0.52	0.011-0.026	0.0018
Third order	0.39-0.51	0.41	0.0013-0.0052	0.0030
Parabolic diffusion	0.94-0.98	0.96	1.26-2.44	1.85
Power function	0.97-0.99	0.98	0.054-0.057	0.055
Simple Elovich	0.92-0.97	0.95	2.04-2.78	2.50

398

399 3.8 Using the parameters of power function model to investigate the effect of treatments on soil
400 Ni desorption

401 As the power function model ($q = at^b$) described the soil Ni release data the best, its
402 parameters (a and b) were used to investigate the effect of biochar application and Si levels on the
403 release of Ni from the Ni-contaminated soil (Table 7). The main effects of biochars and Si levels
404 and their interactions on the 'a' and 'b' parameters were significant ($P < 0.01$). As Dang et al.
405 (1994) reported, in this kinetics model, a decrease in parameter 'a' and an increase in parameter 'b'
406 indicates a decrease in the rate of heavy metals desorption from the soil. The main effects of
407 treatments showed that addition of all the biochar treatments caused a significant decrease in the
408 'a' parameter compared to the control while the 'b' parameter was significantly increased (Table
409 7). The same trend was observed for all the Si treatment rates (Table 7). Therefore, it can be
410 concluded that the use of all the biochars and Si levels has caused a decrease in the rate of Ni
411 release from the Ni-contaminated soil. Generally, there was a greater decrease in Ni desorption in
412 biochar treatments prepared at the higher temperature (Table 7). The interaction effects indicated
413 that the most effective combined treatment in reducing the rate of Ni release from the soil was
414 SM500+S₂ which had the lowest value of parameter 'a' (4.52) and the highest value of parameter
415 'b' (0.264) among the treatments.

416 If it is differentiated from the power function equation ($q = at^b$) with respect to time (t)
417 ($dq/dt = ab t^{b-1}$), when $t = 1$ s = 0, the ratio of dq/dt becomes 'ab'. This parameter indicates the
418 amount of heavy metal desorption in the initial time (Dalal, 1985). The 'ab' parameter was affected
419 by the application of Si levels and biochars, so that this parameter was significantly decreased
420 compared to the control with addition of all the biochars (12.4%, 24.2%, 15.4% and 21.3% for the
421 SM300, SM500, RH300 and RH500, respectively) and Si rates (13% from S₀ to S₂), (Table 7).
422 This finding also confirmed the effect of applied treatments in reducing the amount of Ni release.
423 The greatest reduction was observed in the combined treatment of SM500+S₂ by 33.5% compared
424 to the control (Table 7).

425

426

427

428



Table 7

The coefficients of power function model as affected by biochars and silicon levels in a Ni-polluted calcareous soil after corn cultivation.

	C	SM300	SM500	RH300	RH500	
	a (mg Cd kg⁻¹ h⁻¹)^b					
S ₀	9.15 a	7.39 c	5.56 gh	6.49 e	5.95 f	6.91 A
S ₁	7.92 b	6.01 f	5.23 i	5.66 g	5.21 i	6.00 B
S ₂	6.90 d	5.39 hi	4.52 k	5.22 i	4.84 j	5.38 C
Mean	7.99 A	6.27 B	5.11 E	5.80 C	5.34 D	
	b (mg Cd kg⁻¹)⁻¹					
S ₀	0.196 i	0.222 g	0.247 d	0.238 e	0.237 e	0.228 C
S ₁	0.212 h	0.238 e	0.246 d	0.250 cd	0.254 bc	0.240 B
S ₂	0.230 f	0.254 bc	0.264 a	0.256 b	0.262 a	0.253 A
Mean	0.212 E	0.238 D	0.252 A	0.248 B	0.251 AB	
	ab					
S ₀	1.79 a	1.68 c	1.37 h	1.54 e	1.41 g	1.55 A
S ₁	1.69 b	1.43 f	1.29 k	1.41 fg	1.32 j	1.42 B
S ₂	1.59 d	1.37 h	1.19 m	1.34 i	1.27 l	1.35 C
Mean	1.69 A	1.48 B	1.28 E	1.43 C	1.33 D	

Notes: C, control; SM300, sheep manure biochar produced at 300°C; SM500, sheep manure biochar produced at 500°C; RH300, rice husk biochar produced at 300°C; RH500, rice husk biochar produced at 500°C; S₀, without Si addition; S₁, application of 250 mg Si kg⁻¹ soil; S₂, application of 500 mg Si kg⁻¹ soil.

* Numbers followed by same letters in each column and rows, in each section, are not significantly (P<0.05) different

The correlation between the parameters of the fitted power function model with soil Ni-chemical fractions, shoot Ni content and soil pH are shown in Table 8. The 'a' and 'ab' parameters had a positive correlation with the soil WsEx, OM and MnOx Ni fractions, while there was a negative correlation among the 'a' and 'ab' parameters the AFeOx and CFeOx Ni fractions. This trend was inverse for the 'b' parameter of the power function model. These correlations verified that the application of silicon and biochar to the Ni-contaminated calcareous soil led to a decrease in the rate and amount of Ni release from the soil by reducing the Ni concentration in chemical forms with higher bioavailability including WsEx, OM and MnOx. Furthermore, the 'a' and 'ab' parameters were negatively correlated with soil pH. Whereas there were positive correlations between these parameters and shoot Ni concentration (Table 8). These findings once again confirmed that the increase in soil pH due to the application of silicon and biochar can cause a decrease in the bioavailability of soil Ni and, as a result, a decrease in the concentration of Ni in aerial parts of the plant.

Table 8

The correlation coefficients (r) between the power function model parameters (a, b, ab) and soil Ni chemical fractions, shoot Ni concentration and soil pH.

	WsEx	Car	OM	MnOx	AFeOx	CFeOx	Res	Shoot Ni Concentration	Soil pH
a	0.63**	0.02 ^{ns}	0.70**	0.53**	-0.44**	-0.80**	0.27 ^{ns}	0.62**	-0.52**
b	-0.59**	0.03 ^{ns}	-0.68**	-0.54**	0.46**	0.83**	-0.28 ^{ns}	-0.63**	0.51**
ab	0.68**	0.04 ^{ns}	0.74**	0.46**	-0.46**	-0.80**	0.29 ^{ns}	0.06**	-0.51**

Notes: WsEx, water soluble and exchangeable fraction; OM, organic fraction; MnOx, bound to manganese oxides; AFeOx, bound to amorphous iron oxides; CFeOx, bound to crystalline iron oxides; Res, residual fraction.

** and ^{ns} indicate significance at the 0.01 probability level and non-significant, respectively.

443



444 **4 Conclusions**

445 The application of biochars and Si in the present study resulted in the transformation of Ni
446 in the soil from more bioavailable and mobile fractions (WsEx, MnOx, OM) to more stable forms
447 (AFeOx and CFeOx). These changes were particularly evident in the WsEx fraction when SM
448 biochars were applied in conjunction with silicon, indicating a strong synergistic effect related to
449 soil pH increase. Application of all biochars and Si reduced DPTA-extractable Ni release from the
450 soil, which was most strongly associated with the increase in CFeOx fraction. Application of all
451 biochars and Si decreased corn Ni uptake, with the combined SM500+S₂ being the most effective.
452 The decrease in corn uptake was correlated with the decrease in the WsEx-Ni fraction and increase
453 in CFeOx fraction. SM500 was likely the most effective biochar due to its higher alkalinity and
454 ash content, and lower acidic functional group content which enhanced Ni sorption reactions with
455 Si. Future research is needed to better understand the mechanisms underlying the interaction
456 effects of Si and biochar application on the distribution of soil Ni chemical forms and to optimize
457 Si application strategies for sustainable Ni management in agricultural and natural ecosystems.

458 **Authors' Contributions** H.R.B. Conceptualization, Formal analysis, Methodology, Investigation,
459 Validation A.G.H. Writing - Review & Editing M.N. Project administration, Visualization E.B.
460 Review & Editing E. F. Laboratory analyses.

461 **Financial support.** No funding was received for conducting this study.

462 **Competing interests.** The contact author has declared that neither they nor their co-authors have
463 any competing interests.

464 **Data availability.** The data generated in this study are available from the corresponding authors
465 upon reasonable request.

466 **Disclaimer.** Publisher's note: Copernicus Publications remains neutral with regard to
467 jurisdictional claims in published maps and institutional affiliations.

468 **Acknowledgements:** This work was supported by College of Agriculture and Natural Resources of Darab,
469 Shiraz University, Darab, Iran.

470 **References**

- 471 Adrees, M., Ali, S., Rizwan, M., Zia-ur-Rehman, M., Ibrahim, M., Abbas, F., Farid, M., Qayyum, M. F.,
472 and Irshad, M. K.: Mechanisms of silicon-mediated alleviation of heavy metal toxicity in plants: a
473 review, *Ecotoxicology and Environmental Safety*, 119, 186-197, 2015.
- 474 Anand, A., Gautam, S., and Ram, L. C.: Feedstock and pyrolysis conditions affect suitability of biochar for
475 various sustainable energy and environmental applications, *Journal of Analytical and Applied*
476 *Pyrolysis*, 170, 105881, 2023.
- 477 Ankita Rao, K., Nair, V., Divyashri, G., Krishna Murthy, T., Dey, P., Samrat, K., Chandraprabha, M., and
478 Hari Krishna, R.: Role of Lignocellulosic Waste in Biochar Production for Adsorptive Removal of
479 Pollutants from Wastewater, in: *Advanced and Innovative Approaches of Environmental*
480 *Biotechnology in Industrial Wastewater Treatment*, Springer, 221-238, 2023.
- 481 Antoniadis, V., Levizou, E., Shaheen, S. M., Ok, Y. S., Sebastian, A., Baum, C., Prasad, M. N., Wenzel,
482 W. W., and Rinklebe, J.: Trace elements in the soil-plant interface: Phytoavailability, translocation,
483 and phytoremediation—A review, *Earth-Science Reviews*, 171, 621-645, 2017.



- 484 Bandara, T., Franks, A., Xu, J., Bolan, N., Wang, H., and Tang, C.: Chemical and biological immobilization
485 mechanisms of potentially toxic elements in biochar-amended soils, *Critical Reviews in*
486 *Environmental Science and Technology*, 50, 903-978, 2020.
- 487 Belton, D. J., Deschaume, O., and Perry, C. C.: An overview of the fundamentals of the chemistry of silica
488 with relevance to biosilicification and technological advances, *The FEBS journal*, 279, 1710-1720,
489 2012.
- 490 Bharti, K. P., Pradhan, A. K., Singh, M., Beura, K., Behera, S. K., and Paul, S. C.: Effect of mycorrhizal
491 co-Inoculation with selected rhizobacteria on soil zinc dynamics, *International Journal of Current*
492 *Microbiology and Applied Sciences*, 7, 1961-1970, 2018.
- 493 Bhat, J. A., Shivaraj, S., Singh, P., Navadagi, D. B., Tripathi, D. K., Dash, P. K., Solanke, A. U., Sonah,
494 H., and Deshmukh, R.: Role of silicon in mitigation of heavy metal stresses in crop plants, *Plants*,
495 8, 71, 2019.
- 496 Boostani, H., Hardie, A., Najafi-Ghiri, M., and Khalili, D.: Investigation of cadmium immobilization in a
497 contaminated calcareous soil as influenced by biochars and natural zeolite application, *International*
498 *Journal of Environmental Science and Technology*, 15, 2433-2446, 2018.
- 499 Boostani, H. R., Hardie, A. G., and Najafi-Ghiri, M.: Chemical fractions, mobility and release kinetics of
500 Cadmium in a light-textured calcareous soil as affected by crop residue biochars and Cd-
501 contamination levels, *Chemistry and Ecology*, 1-14, 2023a.
- 502 Boostani, H. R., HARDIE, A. G., and NAJAFI-GHIRI, M.: Lead stabilization in a polluted calcareous soil
503 using cost-effective biochar and zeolite amendments after spinach cultivation, *Pedosphere*, 33, 321-
504 330, 2023b.
- 505 Boostani, H. R., Najafi-Ghiri, M., and Mirsoleimani, A.: The effect of biochars application on reducing the
506 toxic effects of nickel and growth indices of spinach (*Spinacia oleracea* L.) in a calcareous soil,
507 *Environmental Science and Pollution Research*, 26, 1751-1760, 2019a.
- 508 Boostani, H. R., Hardie, A. G., Najafi-Ghiri, M., and Khalili, D.: The effect of soil moisture regime and
509 biochar application on lead (Pb) stabilization in a contaminated soil, *Ecotoxicology and*
510 *Environmental Safety*, 208, 111626, 2021.
- 511 Boostani, H. R., Hardie, A. G., Najafi-Ghiri, M., and Zare, M.: Chemical speciation and release kinetics of
512 Ni in a Ni-contaminated calcareous soil as affected by organic waste biochars and soil moisture
513 regime, *Environmental Geochemistry and Health*, 45, 199-213, 2023c.
- 514 Boostani, H. R., Najafi-Ghiri, M., Amin, H., and Mirsoleimani, A.: Zinc desorption kinetics from some
515 calcareous soils of orange (*Citrus sinensis* L.) orchards, southern Iran, *Soil science and plant*
516 *nutrition*, 65, 20-27, 2019b.
- 517 Chatterjee, R., Sajjadi, B., Chen, W.-Y., Mattern, D. L., Hammer, N., Raman, V., and Dorris, A.: Effect of
518 pyrolysis temperature on physicochemical properties and acoustic-based amination of biochar for
519 efficient CO₂ adsorption, *Frontiers in Energy Research*, 8, 85, 2020.
- 520 Claoston, N., Samsuri, A., Ahmad Husni, M., and Mohd Amran, M.: Effects of pyrolysis temperature on
521 the physicochemical properties of empty fruit bunch and rice husk biochars, *Waste Management*
522 *& Research*, 32, 331-339, 2014.
- 523 Dalal, R.: Comparative prediction of yield response and phosphorus uptake from soil using anion-and
524 cation-anion-exchange resins, *Soil Science*, 139, 227-231, 1985.
- 525 Dang, Y., Dalal, R., Edwards, D., and Tiller, K.: Kinetics of zinc desorption from Vertisols, *Soil Science*
526 *Society of America Journal*, 58, 1392-1399, 1994.
- 527 Deng, Y., Huang, S., Laird, D. A., Wang, X., and Meng, Z.: Adsorption behaviour and mechanisms of
528 cadmium and nickel on rice straw biochars in single-and binary-metal systems, *Chemosphere*, 218,
529 308-318, 2019.
- 530 Derakhshan Nejad, Z., Jung, M. C., and Kim, K.-H.: Remediation of soils contaminated with heavy metals
531 with an emphasis on immobilization technology, *Environmental geochemistry and health*, 40, 927-
532 953, 2018.
- 533 Dey, D., Sarangi, D., and Mondal, P.: Biochar: Porous Carbon Material, Its Role to Maintain Sustainable
534 Environment, in: *Handbook of Porous Carbon Materials*, Springer, 595-621, 2023.



- 535 El-Naggar, A., Rajapaksha, A. U., Shaheen, S. M., Rinklebe, J., and Ok, Y. S.: Potential of biochar to
536 immobilize nickel in contaminated soils, in: *Nickel in Soils and Plants*, CRC Press, 293-318, 2018.
- 537 El-Naggar, A., Chang, S. X., Cai, Y., Lee, Y. H., Wang, J., Wang, S.-L., Ryu, C., Rinklebe, J., and Ok, Y.
538 S.: Mechanistic insights into the (im) mobilization of arsenic, cadmium, lead, and zinc in a multi-
539 contaminated soil treated with different biochars, *Environment International*, 156, 106638, 2021.
- 540 Flore, G., Catherine, K., and Jean-Dominique, M.: Benefits of plant silicon for crops: a review *Agron*,
541 *Sustain. Dev.*, 32, 201-213, 2012.
- 542 Gao, W., He, W., Zhang, J., Chen, Y., Zhang, Z., Yang, Y., and He, Z.: Effects of biochar-based materials
543 on nickel adsorption and bioavailability in soil, *Scientific Reports*, 13, 5880, 2023.
- 544 Ghasemi-Fasaei, R., Maftoun, M., Ronaghi, A., Karimian, N., Yasrebi, J., Assad, M., and Ippolito, J.:
545 Kinetics of copper desorption from highly calcareous soils, *Communications in Soil Science and*
546 *Plant Analysis*, 37, 797-809, 2006.
- 547 Hossain, M. A., Piyatida, P., da Silva, J. A. T., and Fujita, M.: Molecular mechanism of heavy metal toxicity
548 and tolerance in plants: central role of glutathione in detoxification of reactive oxygen species and
549 methylglyoxal and in heavy metal chelation, *Journal of botany*, 2012, 2012.
- 550 Ippolito, J., Berry, C., Strawn, D., Novak, J., Levine, J., and Harley, A.: Biochars reduce mine land soil
551 bioavailable metals, *Journal of environmental quality*, 46, 411-419, 2017.
- 552 Kamali, S., Ronaghi, A., and Karimian, N.: Soil zinc transformations as affected by applied zinc and organic
553 materials, *Communications in soil science and plant analysis*, 42, 1038-1049, 2011.
- 554 Keiluweit, M., Nico, P. S., Johnson, M. G., and Kleber, M.: Dynamic molecular structure of plant biomass-
555 derived black carbon (biochar), *Environmental science & technology*, 44, 1247-1253, 2010.
- 556 Li, X.: Technical solutions for the safe utilization of heavy metal-contaminated farmland in China: a critical
557 review, *Land Degradation & Development*, 30, 1773-1784, 2019.
- 558 Liang, Y., Wong, J., and Wei, L.: Silicon-mediated enhancement of cadmium tolerance in maize (*Zea mays*
559 *L.*) grown in cadmium contaminated soil, *Chemosphere*, 58, 475-483, 2005.
- 560 Lindsay, W. L. and Norvell, W.: Development of a DTPA soil test for zinc, iron, manganese, and copper,
561 *Soil science society of America journal*, 42, 421-428, 1978.
- 562 Liu, L., Guo, X., Wang, S., Li, L., Zeng, Y., and Liu, G.: Effects of wood vinegar on properties and
563 mechanism of heavy metal competitive adsorption on secondary fermentation based composts,
564 *Ecotoxicology and environmental safety*, 150, 270-279, 2018.
- 565 Lu, K., Yang, X., Gielen, G., Bolan, N., Ok, Y. S., Niazi, N. K., Xu, S., Yuan, G., Chen, X., and Zhang,
566 X.: Effect of bamboo and rice straw biochars on the mobility and redistribution of heavy metals
567 (Cd, Cu, Pb and Zn) in contaminated soil, *Journal of environmental management*, 186, 285-292,
568 2017.
- 569 Ma, C., Ci, K., Zhu, J., Sun, Z., Liu, Z., Li, X., Zhu, Y., Tang, C., Wang, P., and Liu, Z.: Impacts of
570 exogenous mineral silicon on cadmium migration and transformation in the soil-rice system and on
571 soil health, *Science of the Total Environment*, 759, 143501, 2021.
- 572 Ma, J. F. and Yamaji, N.: Silicon uptake and accumulation in higher plants, *Trends in plant science*, 11,
573 392-397, 2006.
- 574 Mailakeba, C. D. and BK, R. R.: Biochar application alters soil Ni fractions and phytotoxicity of Ni to
575 pakchoi (*Brassica rapa L. ssp. chinensis L.*) plants, *Environmental Technology & Innovation*, 23,
576 101751, 2021.
- 577 Maruyama, M., Sawada, K. P., Tanaka, Y., Okada, A., Momma, K., Nakamura, M., Mori, R., Furukawa,
578 Y., Sugiura, Y., and Tajiri, R.: Quantitative analysis of calcium oxalate monohydrate and dihydrate
579 for elucidating the formation mechanism of calcium oxalate kidney stones, *Plos one*, 18, e0282743,
580 2023.
- 581 Myszk, B., Schüßler, M., Hurle, K., Demmert, B., Detsch, R., Boccaccini, A. R., and Wolf, S. E.: Phase-
582 specific bioactivity and altered Ostwald ripening pathways of calcium carbonate polymorphs in
583 simulated body fluid, *RSC advances*, 9, 18232-18244, 2019.
- 584 Nasrabadi, M., Omid, M. H., and Mazdeh, A. M.: Experimental Study of Flow Turbulence Effect on
585 Cadmium Desorption Kinetics from Riverbed Sands, *Environmental Processes*, 9, 10, 2022.



- 586 Okolo, C. C., Gebresamuel, G., Zenebe, A., Haile, M., Orji, J. E., Okebalama, C. B., Eze, C. E., Eze, E.,
587 and Eze, P. N.: Soil organic carbon, total nitrogen stocks and CO₂ emissions in top-and subsoils
588 with contrasting management regimes in semi-arid environments, *Scientific Reports*, 13, 1117,
589 2023.
- 590 Page, A., Miller, R., and Keeney, D.: *Methods of soil analysis, part 2, Chemical and microbiological*
591 *properties*, 2, 643-698, 1982.
- 592 Poznanović Spahić, M. M., Sakan, S. M., Glavaš-Trbić, B. M., Tančić, P. I., Škrivanj, S. B., Kovačević, J.
593 R., and Manojlović, D. D.: Natural and anthropogenic sources of chromium, nickel and cobalt in
594 soils impacted by agricultural and industrial activity (Vojvodina, Serbia), *Journal of Environmental*
595 *Science and Health, Part A*, 54, 219-230, 2019.
- 596 Rizwan, M., Ali, S., Qayyum, M. F., Ibrahim, M., Zia-ur-Rehman, M., Abbas, T., and Ok, Y. S.:
597 Mechanisms of biochar-mediated alleviation of toxicity of trace elements in plants: a critical
598 review, *Environmental Science and Pollution Research*, 23, 2230-2248, 2016.
- 599 Saffari, M., Karimian, N., Ronaghi, A., Yasrebi, J., and Ghasemi-Fasaei, R.: Stabilization of nickel in a
600 contaminated calcareous soil amended with low-cost amendments, *Journal of soil science and plant*
601 *nutrition*, 15, 896-913, 2015.
- 602 Sajadi Tabar, S. and Jalali, M.: Kinetics of Cd release from some contaminated calcareous soils, *Natural*
603 *resources research*, 22, 37-44, 2013.
- 604 Shahzad, B., Tanveer, M., Rehman, A., Cheema, S. A., Fahad, S., Rehman, S., and Sharma, A.: Nickel;
605 whether toxic or essential for plants and environment-A review, *Plant Physiology and*
606 *Biochemistry*, 132, 641-651, 2018.
- 607 Shen, B., Wang, X., Zhang, Y., Zhang, M., Wang, K., Xie, P., and Ji, H.: The optimum pH and Eh for
608 simultaneously minimizing bioavailable cadmium and arsenic contents in soils under the organic
609 fertilizer application, *Science of the Total Environment*, 711, 135229, 2020.
- 610 Singh, J., Karwasra, S., and Singh, M.: Distribution and forms of copper, iron, manganese, and zinc in
611 calcareous soils of India, *Soil Science*, 146, 359-366, 1988.
- 612 Sun, L., Zhang, G., Li, X., Zhang, X., Hang, W., Tang, M., and Gao, Y.: Effects of biochar on the
613 transformation of cadmium fractions in alkaline soil, *Heliyon*, e12949, 2023.
- 614 Sun, Y., Gao, B., Yao, Y., Fang, J., Zhang, M., Zhou, Y., Chen, H., and Yang, L.: Effects of feedstock type,
615 production method, and pyrolysis temperature on biochar and hydrochar properties, *Chemical*
616 *engineering journal*, 240, 574-578, 2014.
- 617 Tomczyk, A., Sokołowska, Z., and Boguta, P.: Biochar physicochemical properties: pyrolysis temperature
618 and feedstock kind effects, *Reviews in Environmental Science and Bio/Technology*, 19, 191-215,
619 2020.
- 620 Vickers, N. J.: Animal communication: when i'm calling you, will you answer too?, *Current biology*, 27,
621 R713-R715, 2017.
- 622 Xiao, Z., Peng, M., Mei, Y., Tan, L., and Liang, Y.: Effect of organosilicone and mineral silicon fertilizers
623 on chemical forms of cadmium and lead in soil and their accumulation in rice, *Environmental*
624 *Pollution*, 283, 117107, 2021.
- 625 Yan, G.-c., Nikolic, M., YE, M.-j., Xiao, Z.-x., and LIANG, Y.-c.: Silicon acquisition and accumulation in
626 plant and its significance for agriculture, *Journal of Integrative Agriculture*, 17, 2138-2150, 2018.
- 627 Yuan, J.-H., Xu, R.-K., and Zhang, H.: The forms of alkalis in the biochar produced from crop residues at
628 different temperatures, *Bioresource technology*, 102, 3488-3497, 2011.
- 629 Zemnukhova, L. A., Panasenko, A. E., Artem'yanov, A. P., and Tsoy, E. A.: Dependence of porosity of
630 amorphous silicon dioxide prepared from rice straw on plant variety, *BioResources*, 10, 3713-3723,
631 2015.
- 632 Zeng, X., Xiao, Z., Zhang, G., Wang, A., Li, Z., Liu, Y., Wang, H., Zeng, Q., Liang, Y., and Zou, D.:
633 Speciation and bioavailability of heavy metals in pyrolytic biochar of swine and goat manures,
634 *Journal of Analytical and Applied Pyrolysis*, 132, 82-93, 2018.
- 635 Zhao, S.-X., Ta, N., and Wang, X.-D.: Effect of temperature on the structural and physicochemical
636 properties of biochar with apple tree branches as feedstock material, *Energies*, 10, 1293, 2017.

<https://doi.org/10.5194/egusphere-2023-2687>

Preprint. Discussion started: 12 January 2024

© Author(s) 2024. CC BY 4.0 License.



637 Zhu, Q., Wu, J., Wang, L., Yang, G., and Zhang, X.: Effect of biochar on heavy metal speciation of paddy
638 soil, *Water, Air, & Soil Pollution*, 226, 1-10, 2015.
639